Hernia (2023) 27:999–1015
https://doi.org/10.1007/s10029-023-02740-z

ORIGINAL ARTICLE

Different cellular and immunohistochemical abdominal wall cicatrization parameters evaluation in comparison with sublay, onlay, and ipom technique in an experimental rat model

F. Ponce Leon[1] · C. M. Takiya[2] · J. R. da Costa[3] · N. B. de Oliveira Santos[1] · J. E. F. Manso[3]

Received: 26 September 2022 / Accepted: 1 January 2023 / Published online: 18 January 2023

Abstract

Purpose Incisional hernia (IH) occurs when there is a partial or complete solution of continuity of a fascia previously incised. Systematic reviews demonstrate that surgical treatment of IHs with the use of meshes are approximately 16%. Meta-analyses have demonstrated the superiority of mesh placement using sublay technique, but without a pathophysiological explanation. Thus, we aim to evaluate the different techniques of mesh positioning in an experimental model.

Methods Fifty rats were distributed into five groups; control; simulation (SM)—submitted to laparotomy only; onlay—the mesh was positioned in onlay fashion; retromuscular (SL)—the mesh was positioned in a sublay fashion; intraperitoneal (IPOM)—positioning of the mesh adjacent to the transversalis fascia, inside the cavity. After 60 days, adhesions, tensiometry, histology, and immunohistochemistry were addressed.

Results The IPOM group had the most adhesions, together with the SL group, with significantly relevant results. The SL group had higher values of tensiometric evaluation, while the IPOM group had the lowest mean in the tensiometry evaluation, being even lower than the SM group. Regarding histological and immunohistochemical findings, the SL group had a higher pixel number count compared to the groups, with statistical significance, in addition to higher expression of polymorphonuclear infiltrate and CD68 markers.

Conclusion The mesh positioning in sublay compartment is associated with the development of more pronounce minimum tensile force required for detaching the surrounding abdominal wall tissues it was incorporated. The intensity of these findings correlates to the different histological and immunohistochemical profiles observed following each repair, since SL group was characterized by a higher proportion of collagen, inflammatory, and reparative elements. Characterizing these pro-healing elements and its counterparts will allow the development of new therapeutic tools which could be added to the still far-from-ideal current therapeutic options for IH treatment.

Keywords Retrorectus · Sublay · IPOM · Onlay · Collagen · Fibroblasts

✉ F. Ponce Leon
fernando.ponceleon@gmail.com

C. M. Takiya
takiyacm@biof.ufrj.br

J. R. da Costa
juliana.jcosta1@gmail.com

N. B. de Oliveira Santos
dranathaliabarros@gmail.com

J. E. F. Manso
mansojef@gmail.com

[1] Division of Abdominal Wall Surgery, Federal University of Rio de Janeiro, Rio de Janeiro, Brazil

[2] Institute of Biophysics Carlos Chagas Filho, Federal University of Rio de Janeiro, Rio de Janeiro, Brazil

[3] Department of Experimental Surgery, Federal University of Rio de Janeiro, Rio de Janeiro, Brazil

Introduction

An incisional hernia (IH) occurs when there is a partial or total discontinuity of a previously incised and sutured fascia, allowing the extrusion of contents through the defect on the aponeurosis [1]. Despite the high prevalence of this disease, results of the available therapeutic options are still poor, and recurrence rates following surgical repairs are higher than 15% even in high-quality specialized centers [2–4].

The mechanism of IH development is multifactorial. Associated risk factors include obesity, old age, malnutrition, inefficient metabolism, due to inadequate digestion and/or assimilation of nutrients, pregnancy, dialysis, and previous infections. Irrespective of the cause, a common pathophysiology implicated in hernia development involves defective repair response, resulting in a poor wound-healing substrate and insufficient collagen deposition [5].

Many surgical strategies are available for IH repairs, and although the choice of the technique will depend on many variables such as the location and size of the abdominal wall defect, surgeon's expertise, and economic conditions of the institution [6], it is a consensus that mesh application results in much superior results [4]. Mesh placement leads to an intense repair response that results in a dense fibrous tissue with high mechanical resistance, which will prevent the defect from re-occurring [7, 8].

Among locations for mesh fixation, many are the techniques available nowadays. The onlay technique, in which the mesh is placed immediately underneath the subcutaneous tissue layer over the anterior sheath of the rectus abdominis muscle, the sublay technique in which the mesh is placed between the rectus abdominis muscle and its posterior sheath, and the intra-abdominal onlay mesh positioning (IPOM), in which the mesh is fixated in the parietal peritoneum, under thee fascia transversalis. A meta-analysis has shown that techniques placing the mesh under the rectus abdominis muscle are related to lower wound infection rates, fewer early postoperative complications, and decreased hernia recurrences [9].

In line with those findings, a retrospective cohort study demonstrated the superiority of sublay over onlay technique regarding recurrence, without additional risks due to its higher complexity [10]. In addition, a meta-analysis has demonstrated the superiority of this technique concerning postoperative recovery, complications, and relapse rates [11]. Despite the strong clinical evidence favoring sublay technique, the exact mechanism responsible for this superiority is unknown, and as already acknowledged from other examples related to improvements in medical science, including hernia disease itself, a clear understanding of such process will allow the development of better therapeutic options.

Aiming that, here, we performed primary suture, onlay, sublay, and IPOM mesh techniques in healthy animals, and analyzed response following those repairs. We chose to evaluate foreign body reaction, repair strength, intra-abdominal adhesions development, amount, and quality of formed collagen and to characterize the associated anatomopathological substrate since all these parameters are related to wound healing and the intensity of some of them is proportional to the final quality of the repair. Surgical repairs were employed directly on healthy animals, without previous hernia induction, to avoid confounding factors related to hernia development. Our goal is to characterize and evaluate the induced fibrogenesis related to the techniques of treatment of incisional hernias, aiming to understand the pathophysiological process involved and to determine if there is an eventual effective superiority of any technique.

Methods

Animal studies' experimental protocol was submitted to the Ethics Committee for the Use of Animals in Scientific Experimentation of the Health Sciences Center of the Universidade Federal do Rio de Janeiro (CEUA-CCS), registered in the National Council for the Control of Animal Experimentation (CONCEA) under process number 01200.001568/2013-87, and received approval for execution. Fifty Wistar rats weighing between 200 and 400 g were provided by the Experimental Surgery Laboratory of the Department of Surgery of the Universidade Federal do Rio de Janeiro (UFRJ).

They were kept in a specific pathogen-free environment, under standard animal allocation conditions (temperature between 20 and 24 °C, relative humidity around 50–60%, with 12 h of light period and 12 h of dark period), fed with specific feed and water ad libitum.

Surgical procedure

Specimens were randomly divided into five groups containing ten rats each. A different surgical technique was applied to each group: IPOM, in which a dual sided mesh was positioned inside the abdomen and fixed under the *fascia transversalis*; sublay (SL), in which the polypropylene mesh was placed between the posterior sheath of the rectus abdominis muscle and the rectus abdominis muscle; onlay (OL), in which the mesh was placed between the anterior sheath of the rectus abdominis muscle and the subcutaneous tissue; simulation (SM), in which laparotomy was followed by abdominal wall primary closure; and control (CT), in which no surgical procedure was performed.

High-density non-absorbable Parietene® Standard (Medtronic®) polypropylene mesh was used for SL and OL techniques with manufacturer's definitions specifying pores of approximately 1.7 × 1.7 mm diameter and an estimated weight of 75 g/m2. A dual sided mesh Symbotex® Composite, with a visceral side containing porcine collagen coating and a parietal side made of polypropylene, was used for the IPOM technique with manufacturer's definitions specifying the hydration of the mesh before it is use. All animals were exposed to the same environmental conditions during the experiment.

Weight was measured immediately before the surgical procedure, to guarantee a similar drug dosage administration. Anesthesia was achieved using xylazine at the dose of 10 mg/kg and ketamine hydrochloride at the dose of 50 mg/kg via intraperitoneal administration. After that, trichotomy of the anterior abdomen was performed and the operative site was prepared with 4% chlorhexidine digluconate, followed by 2% alcoholic chlorhexidine solution.

The surgical procedure was performed under sterile conditions. A 4-cm midline incision was made, and dissection was performed, reaching the abdominal cavity. In rats allocated to the IPOM group, dissection of the space between the anterior sheath of the rectus abdominis muscle and the subcutaneous tissue was performed bilaterally, generating flaps. Later, a dual mesh of standard size of 2.5 × 2.5 cm was correctly positioned after proper hydration and sutured with polyglactin 910 4.0 transfixing stitches. Then the aponeurosis was sutured with a running suture of polyglactin 910 4.0. Afterward, skin synthesis with non-absorbable polyamide 4.0 was performed.

In rats allocated to the sublay model, the precepts published by Chevrel et al. and Rivers et al. were followed [12, 13]. Briefly, dissection of the posterior sheath of the rectus abdominis muscle was performed bilaterally, generating flaps, which were sutured with absorbable polyglactin 910 4.0. Then a polypropylene mesh of standard size 2.5 × 2.5 cm was placed over the posterior sheath and fixed with four single stitches of polyglactin 910 4.0 (Vicryl®, Ethicon). The anterior sheath of the rectus abdominis was then closed with polyglactin 910 4.0, followed by synthesis of the skin with polyamide 4.0 (Mononylon®, Ethicon).

In rats allocated to the onlay group, dissection of the space between the anterior sheath of the rectus abdominis muscle and the subcutaneous tissue was performed bilaterally, generating flaps, which were sutured with polyglactin 910 4.0. Then a polypropylene mesh of standard size of 2.5 × 2.5 cm was placed over the anterior sheath and sutured with four single stitches of polyglactin 910 4.0. Afterward, skin synthesis with non-absorbable polyamide 4.0 was performed. Figure 1 shows the final aspect of the mesh implanted in the abdominal wall of OL and SL subjects, and the final aspect of the IPOM technique implanted mesh (Fig. 1).

In rats allocated to the simulation group, synthesis of the abdominal wall was performed with polyglactin 910 4.0, followed by synthesis of the skin with polyamide 4.0. Operative procedures were performed in a systematic way, with surgical times ranging from 10 min to a maximum of 35 min. Only up to four rats were operated per day, to maintain standardization of the technique.

Since the biological cycle of the rat is faster than that of the human [5], an interval of 60 days between the first surgery and euthanasia was standardized, allowing time enough for the initial phase of scarring to be completed [14], and an ideal integration between aponeurosis and mesh could be achieved. After the surgery, animals were returned to the animal facility under the previously described conditions. Postoperative analgesia consisted of dipyrone at the dose of 90 mg/mL diluted in water and was administered for 3 days.

Rats were euthanized with lethal doses of xylazine and ketamine intraperitoneally, and the abdominal wall was removed in bloc (U shaped). The fragments of abdominal wall were composed of skin, subcutaneous tissue, rectus abdominis muscles with their aponeuroses, polypropylene, or dual mesh (when present according to the technique used) and mesothelium. During abdominal wall extraction, adhesions were evaluated, followed by division of the abdominal wall fragment in three samples, which were then used for

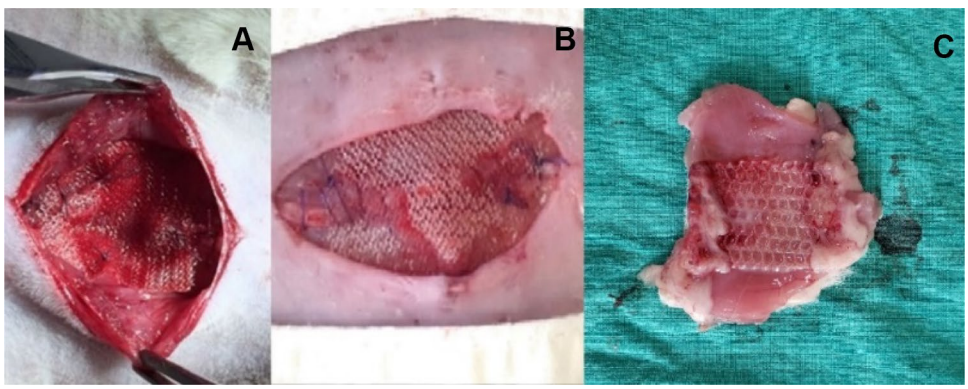

Fig. 1 Final aspect of mesh positioning; **A** Sublay. Addison are holding the upper aponeurosis of the rectus abdominis muscle, and exposing the mesh position between the lower rectus abominis muscle and the rectus abdominis muscle itself, **B** Onlay, **C** Abdominal wall fragment with a mesh positioned in an IPOM technique.

Table 1 Adherence classification according to Ricciardi et al.

Grade	Finding
0	Absence of adhesions
1	Small number of adhesions, easily undone
2	Firm adhesions between bowels, resistant to manipulation, without involvement of the abdominal wall
3	Firm adhesions between the abdominal wall and an organ or structure
4	Firm adhesions between the abdominal wall and more than one organ or structure
5	Firm adhesions between the abdominal wall and more than one organ or structure with enteric fistula

tensiometric analysis, histological and immunohistochemistry evaluation, separately.

Adhesions and tensiometric evaluation

Adhesions were evaluated macroscopically, using a qualitative score according to Ricciardi et al. [15], which classifies them into six different grades as demonstrated in the following table (Table 1).

Tensiometric evaluation was performed using a digital dynamometer with a load cell of 5 kgf, support for traction test and a software for data capture (Lutron Electronic Enterprise Co. Ltd, TW; Instrutherm, São Paulo—BR) from the Experimental Surgery Laboratory of UFRJ. To evaluate the strength of mesh incorporation into the tissue, one side of the fragment was fixed to the base of the tensiometer with a clamp, with the mesh still on the fragment but not attached to the clamp. The contralateral side was grasped on the mesh by a retractable clamp, connected to the dynamometer, which pulled the mesh in the opposite direction to the fixed clamp at a determined speed of 60 mm/min. The minimal tensile strength (MTS) for mesh removal from the surrounding tissue was electronically recorded in Newtons (N). In simulation (laparotomy only) and control (no surgery) groups, one of the aponeurotic borders laterals to the incision was apprehended by each of the clamps, thus assessing the minimal tensile strength (MTS) necessary for the aponeurotic suture to be ruptured by traction. Following this protocol, our goal was to record a parameter that could measure the quality of the surgical repair, concerning recurrence prevention.

Histology

For the microscopical study, a strip of the abdominal wall (transversal section) of about 50 × 10 mm containing the implanted mesh in the center, or from sham-operated animals were harvested and immediately fixed in 10% formaldehyde solution, for about 48 h. Then they were dehydrated in crescent solutions of ethanol, clarified in xylene and embedded in paraffin. Each paraffin block/section was coded to allow a blind evaluation. Sections (5 µm-thick) were cut in a rotatory microtome and stained with hematoxylin–eosin (HE) for topographical description and with a modified *picrosirius* red (PSR) staining for collagen quantification [16].

Immunohistochemistry

For immunohistochemistry, the following primary antibodies were used: mouse monoclonal antibody against rat CD68 (clone ED1, Abd Serotec, BioRad Laboratories, CA, USA, cat n. MCA341GA, 1:100), rabbit polyclonal antibody against mannose receptor (AbCam cat. n. ab64693, 1:100) for macrophages M2, and rabbit polyclonal iNOS (Invitrogen, Thermo-Fisher, CA, USA, cat. n. PA1-036, dilution 1: 100). Briefly, paraffin sections were dewaxed, and rehydrated, submitted to blockage of free aldehyde residues with 50 mM ammonium chloride in phosphate saline buffer (PBS), pH 8.0 for 15 min, permeabilized with 0.5% Triton-X100-PBS solution (15 min), and incubated in a dark ambient with a 3% hydrogen peroxide in methanol (15 min) solution for endogenous peroxidase inhibition. After washing with PBS pH 7.4, sections were submitted to heat-mediated antigen retrieval performed in a microwave (0.01 M acid citric-sodium citrate buffer, pH 6.0 for 3 min). After cooling, sections were incubated with the blocking reagent [5% bovine albumin serum (BSA), 0.005% gelatin, 0.05% Triton X-100, 0.025% Tween 20 in PBS pH 7.4] for 1 h, followed by the incubation of primary antibodies diluted with 3% BSA in PBS, containing 1% of normal goat serum (Sigma-Aldrich, USA) in a dark, humid chamber, overnight at 4 °C. Then after washing with 0.25% Tween–PBS solution (PBS-T), and sections were incubated with the secondary antibodies: Histofine® Simple Stain Rat MAX—PO (Mouse) and—PO (Rabbit) from Nichirei, Japan, cat (414171F and 414181F, respectively, both for rat tissue), for 1 h and peroxidase was revealed with diaminobenzidine (Liquid DAB, Dako, cat. K3468), washed in distilled water and counterstained with hematoxylin. Negative control slides were incubated with mouse or rabbit isotype immunoglobulins or with the antibody diluent solution.

Histomorphometry and histopathological analyses

A computer-assisted image analysis system comprising a Nikon Eclipse E-800 microscope connected to a computer with a digital camera (Evolution, Media Cybernetics Inc., Bethesda, MD) coupled to Q-Capture 2.95.0 software (Silicon Graphic Inc., Milpitas, CA) was used to perform histomorphometrical analyses. Fifteen high-quality photomicrographs (2048 × 1536-pixel buffer) of HE, PSR-stained sections as well as immunostainings (CD68, iNOS and mannose receptor) were captured from non-overlapping areas of the implanted meshes.

Histological assessments of tissue response to the implanted mesh were performed evaluating the numbers of polynucleated cells (polymorphonuclear, eosinophils), myeloid progenitor cells, lymphocytes, plasma cells, fibroblasts, multinucleated giant cells, and the number of vessels in the captured images (15 images/animal) of areas of slides stained with HE, using a 20 × objective lens (fibroblasts, vessels, and giant cells) or 40 × objective lens (inflammatory cells). The collagen network induced by mesh implantation was quantified through images obtained from histological sections stained with modified *picrosirius* red. Fifteen photomicrographs also were obtained using the 40 × objective.

Afterward, fibrosis was assessed through images obtained from PSR-stained sections and the quantification was performed using the ImageJ® software (version 1.53a, National Institutes of Health, USA) for indirect accounting of collagen expression in the samples. Data acquisition and analysis were blinded in all cases.

CD68, mannose receptor, and iNOS surface density

Surface density of these markers were obtained from CD68, mannose receptor, and iNOS-stained sections, as previously described [17]. The results were expressed as the % of stained areas in the total area examined, and results were expressed as median (interquartile range) of the surface density of CD68 (macrophages), mannose receptor (M2), and iNOS (M1).

Statistical analysis

For statistical analysis, GraphPad Prism 5 software (GraphPad Software, Inc., La Jolla, CA, USA) was used. For histological data, results were presented as as median (interquartile range) and evaluated with ANOVA non-parametric test (Kruskal–Wallis) followed by Dunn's multiple comparison test. For adhesions or biomechanical test, univariate ANOVA followed by the Tukey post hoc test when the p value was less than 0.05 in the intergroup assessment. 95% confidence intervals (95% CI) were calculated for the values found and a p value of less than 0.05 was considered an ideal measure to reject the null hypothesis.

Results

None of the 50 rats studied presented any complications throughout the experiment, and there were no deaths. Animals submitted to surgical procedures had a good and predicted postoperative recovery. During the study, no changes in rat behavior, such as weight loss or difficulty in mobilization, were observed. There were no enteric fistulas.

Adhesions analysis

All animals were evaluated for the macroscopic appearance of the intra-abdominal and visceral adhesions in the immediate postmortem. In the IPOM group, six animals had grade 3 adhesion and four animals had grade 4 adhesions, with no animals with grade 0, 1, 2 or 5. In the SL group, one animal had grade 0 adhesions, two animals had grade 1, four animals had grade 3, and three animals had grade 4. There were no animals with grade 2 or 5. In the OL group, three animals had grade 0, six animals had grade 1, and one animal had grade 2. There were no animals with grade 3, 4 or 5. In the SM group, four animals had grade 0 and six animals had grade 1. There were no animals in this group with grade 2, 3, 4 or 5. In the CT group, there were no adhesions. Comparison of adhesion grades between experimental groups revealed that IPOM was associated with a significantly greater intensity of adhesion formation (IPOM: mean 3.4 and standard deviation (SD) 0.54; SL: mean 2.75 and SD 1.16; OL: mean 0.8 and SD 0.63; SM: mean 0.5 and SD 0.52; $p < 0.0001$).

In the univariate multiple comparisons, we can observe that comparing the IPOM and SL groups, we obtain a confidence interval between − 0.37 and 1.67, with a p value of 0.38. Analyzing the IPOM and OL groups, we have a confidence interval that varies from 1.8 to 3.66; with the IPOM and SM groups, we found a confidence interval between 2.13 and 3.99; with the IPOM group vs. the CT group, we have a confidence interval between 2.41 and 4.38; with the SL and OL groups, we obtain a confidence interval between 1.25 and 2.87; with the SL and SM groups, we have a confidence interval between 1.62 and 3.2, and finally, with the SL and CT groups, there is a confidence interval of 1.89 and 3.6. All of them with a p value lower than 0.0001.

Comparing the OL and SM groups, there was a confidence interval that varied between − 0.32 and 0.99, with a p value of 0.6. When comparing the OL and CT groups, the confidence interval measured was − 0.06–1.4 with p of 0.09. Finally, when comparing the SM and CT groups,

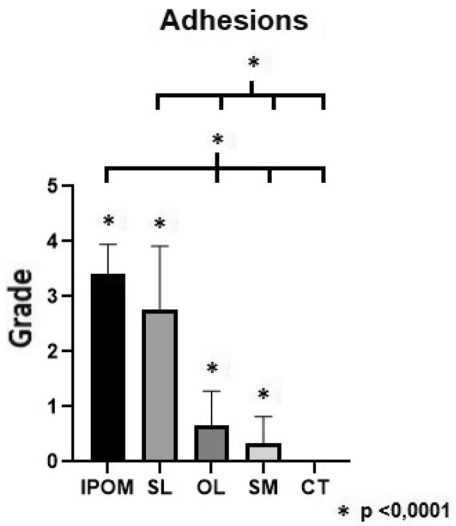

Fig. 2 Adhesion grades

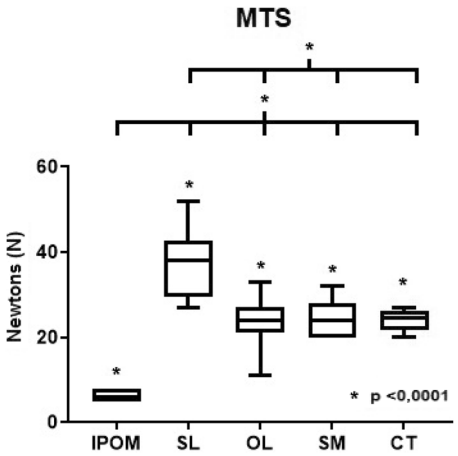

Fig. 3 MTS values found

a confidence interval between − 0.4 and 1.06 was verified, with a *p* value of 0.7. (Fig. 2).

Tensiometric evaluation

Tensiometric evaluation was performed on abdominal wall fragments from all the animals. In IPOM group, measurements of MTS ranged from 5 to 8.14 N, with a mean of 6.58 N and SD of 1.45. In SL group, measurements of MTS ranged from 27 to 52 N, with a mean of 36.75 N and SD of 5.92. In OL group, the range was from 21 to 33 N, with a mean of 26.4 N and SD of 3.5. In SM group, the range was from 20 to 26 N, with a mean of 23 N and SD of 3.39. Finally, in CT group, the range was from 20 to 27, with a mean of 24.1 and SD of 2.51 ($p < 0.0001$).

In the univariate multiple comparison, we can observe that comparing the IPOM and SL groups, we observed a confidence interval between − 38.84 and − 22.96; comparing the IPOM and OL groups, we visualized a confidence interval between − 25.02 and − 10.05; comparing the IPOM and SM groups, we observed a confidence interval between − 25.62 and − 10.65; and comparing the IPOM group vs. CT group, there is a confidence interval between − 25.64 and − 9.75. All of them with a *p* value lower than 0.0001.

Comparing the SL and OL groups, we obtained a confidence interval between 7.44 and 19.29; with the SL and SM groups, a confidence interval between 6.84 and 18.69 was detected; and comparing the SL group with the CT group, we observed a range between 6.71 and 19.68, also with a *p* value lower than 0.0001. Evaluating the OL and SM groups, a confidence interval ranging between − 5.89 and 4.69 was detected, with a *p* value of 0.99. When comparing the OL and CT groups, the confidence interval varied between − 6.08 and 5.75, with a *p* value of above 0.99. Finally, comparing the SM group with the CT group, we observed a range between − 5.48 and 6.35, with a *p* value of 0.99 (Fig. 3).

Histological results

The implantation site of the polypropylene meshes in animals of SL, OL, and IPOM groups showed presence of an intense infiltrate of myeloid cells (polynucleated cells mainly neutrophils, mononuclear cells), and multinucleated giant cells located around mesh fibers, but differing in amount and types within the groups. SL group showed large fibers totally degraded, and the predominant cell type infiltrating the mesh was mononuclear cells followed by neutrophils, and myeloid progenitor cells. In fact, these group of cells were significantly increased in SL group compared to OL group.

The SL group showed a histological evaluation, microscopic analyzes were performed to identify and visualize typical inflammatory infiltrate, polymorphonuclear infiltrate, red pixels count, presence of giant cells, findings compatible with neovascularization and the identification of fibroblasts. The CT and SM groups did not show noteworthy changes in the histological scrutiny, as there were almost no findings in the elements surveyed, and it was chosen not to describe the results extensively.

Polymorphonuclear, lymphocyte, and plasma cells infiltrate

When evaluating the presence of polymorphonuclear infiltrate, we observed in the IPOM group an average of 3.83, with a SD of 0.59, in the SL group an average of 8.26, with a SD of 0.94 and in the OL a mean of 4.46, with a SD of 0.92. When performing univariate multiple comparisons

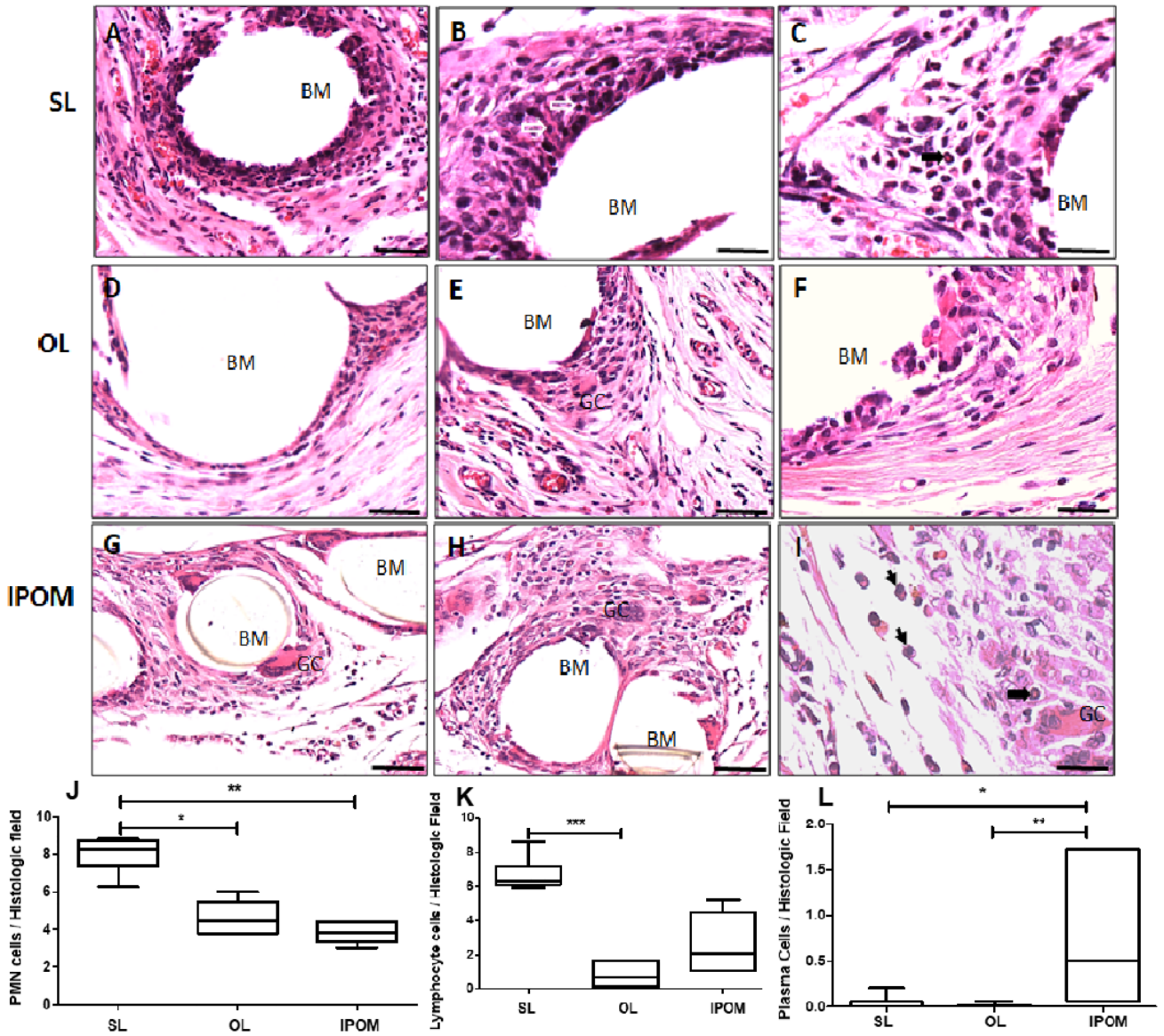

Fig. 4 Polymorphonuclear deposition around mesh—Sublay, Onlay, and IPOM models, (**A**, **D**) and (**G**), respectively. Lymphocyte expression near the mesh region—Sublay, Onlay, and IPOM models, (**B**, **E**) and (**H**), respectively. Plasma cells presentation—Sublay, Onlay, and IPOM models, (**C**, **F**) and (**I**), respectively. H&E. 1:200 µm. Graphics regarding histologic finding of PMN cells, lymphocyte cells, and plasma cells in **J**, **K**, and **L**, respectively. *BM* biomaterial (mesh)

on the typical infiltrate values found, we observed *p* values under 0.05 when comparing the IPOM vs. SL and OL vs. SL groups, with a global *p* value of 0.002 for this group.

In the lymphocyte count performed, we observed in the IPOM group an average of 2.06, with a SD of 1.72; in the SL group, an average of 6.29, with a SD of 0.98 and in the OL group, a mean of 0.69, with a SD of 0.70. When performing univariate multiple comparisons on the typical infiltrate values found, we observed *p* value under 0.05 only when comparing OL vs. SL group, with a global *p* value of 0.001 in this subject.

Analyzing the presence of plasma cells in the analyzed abdominal wall fragments, we can observe in the IPOM group an average of 0.5, with a SD of 0.79 and minimal values in the SL and OL groups that did not generate a substantial analysis. The global *p* value found in one-way ANOVA analysis was 0.0003 regarding and sustaining the fact that only the IPOM technique expressed those type of cells. Figure 4 summarizes the findings described.

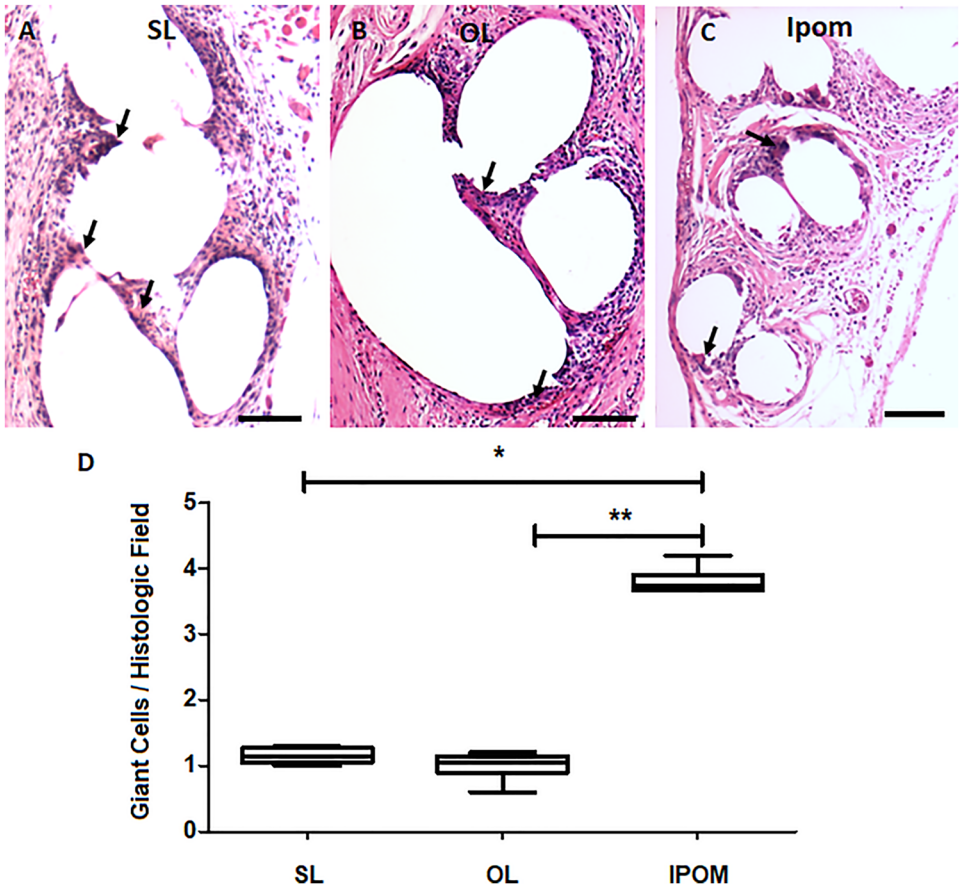

Fig. 5 Statistics regarding giant cells found mononuclear cells deposition final aspect. Arrows demonstrating giant cells. Sublay, Onlay, and IPOM models, (**A**, **B**) and (**C**), respectively. H&E, 1:200 µm. **D** summarizing the statistics of giant cells

Giant cells and red pixels count

Regarding the evaluation of the presence of multinucleated giant cells, we visualized in the IPOM group an average of 3.74, with a SD of 0.2; in the SL group, an average of 1.13, with a SD of 0.11; and in the OL group, an average of 1.06, with a SD of 0.21. When performing univariate multiple comparisons on the giant cell values found, we observed *p* values under 0.05 comparing IPOM vs. SL and IPOM vs. OL groups, with a global *p* value of 0.002 in this analysis (Fig. 5).

Pixel counting was performed on all abdominal walls studied, except for the control group, since the objective of this study does not include the evaluation of the physiological anatomy of the animal model. In the IPOM group, we found an average of 562,540 red pixels, with a SD of 276,362. In the SL group, an average of 897,399 pixels was obtained, with a SD of 214,124. In the OL group, an average of 768,463 red pixels was observed, with a SD of 69,517 and in the SM group, an average of 833,257 pixels, with a SD of 178,769 was observed. Comparing the values found, after the pre-test evaluations and the post-test corrections, a *p* value of 0.001 was determined.

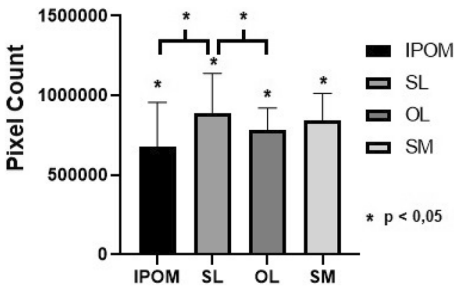

Fig. 6 Red pixels' count

In the univariate multiple comparisons, we can observe that when comparing the IPOM and SL groups, we obtain a confidence interval between − 352,163 and − 60,478, with a *p* value of 0.001. Evaluating the IPOM and OL groups, we visualize a confidence interval between − 244,942 and 45,245, with a *p* value of 0.28. When analyzing the IPOM and SM groups, we observed a confidence interval between − 324,381 and 3163, with a value of 0.056. When investigating the SL and OL groups, we obtained a confidence interval between 35.55 and 212,909, with a *p* value of 0.04. Analyzing the SL and SM groups, a confidence interval

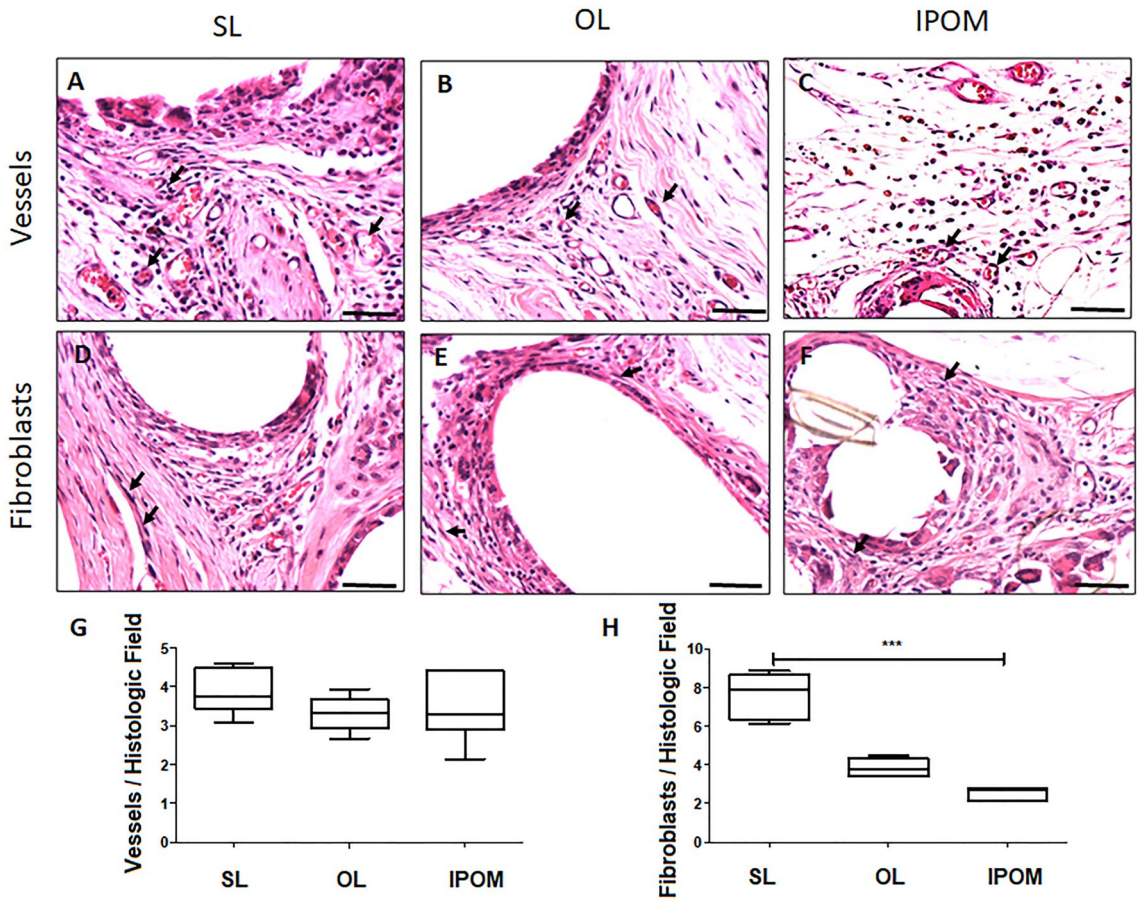

Fig. 7 Summary of neovascularization and fibroblast expression. Arrows denoting vessels. Sublay model, (**A**) and (**D**). Onlay model, (**B**) and (**E**). IPOM model, (**C**) and (**F**). H&E. 1:200 µm. Graphic regarding statistics found for neovascularization and fibroblasts is shown in (**G**) and (**H**), respectively

between − 85,047 and 176,471 was detected, with a *p* value of 0.8, and finally, when evaluating the OL group with the SM group, we observed an interval between − 190,683 and 69,163, with a *p* value of 0.61 (Fig. 6).

Neovascularization and fibroblasts

When evaluating the presence of neovascularization, we observed in the IPOM group an average of 3.3, with a SD of 0.86; in the SL group, an average of 3.76, with a SD of 0.58 and in the OL group, a mean of 3.33, with a SD of 0.46. When performing univariate multiple comparisons of the neovascularization values found, we observed no significant statistics between the groups, with a *p* value of 0.27.

Analyzing the presence of fibroblasts in the analyzed abdominal wall fragments, we can observe in the IPOM group an average of 2.73, with a SD of 0.32, in the SL group, an average of 7.86, with a SD of 1.16, and in the OL group, an average of 3.76, with a SD of 0.46. When evaluating the univariate multiple comparisons of the values of fibroblasts expressed, we found *p* value under 0.05 only comparing the IPOM vs. SL group, with a global *p* value of 0.0005. Figure 7 demonstrates the findings above.

Immunohistochemistry

The immunohistochemical analysis comprised the evaluation of the expression of markers CD 68, mannose receptors, iNOS, and collagen density, using the average expression in the microscopic analysis, in percentage referring to the 40-times magnification field. The CT group did not show noteworthy changes in immunohistochemical detail, as there were almost no findings in the elements surveyed, and we chose not to describe the results extensively.

CD 68

When evaluating the presence of markers for CD 68, we observed in the IPOM group an average of 2.57%, with

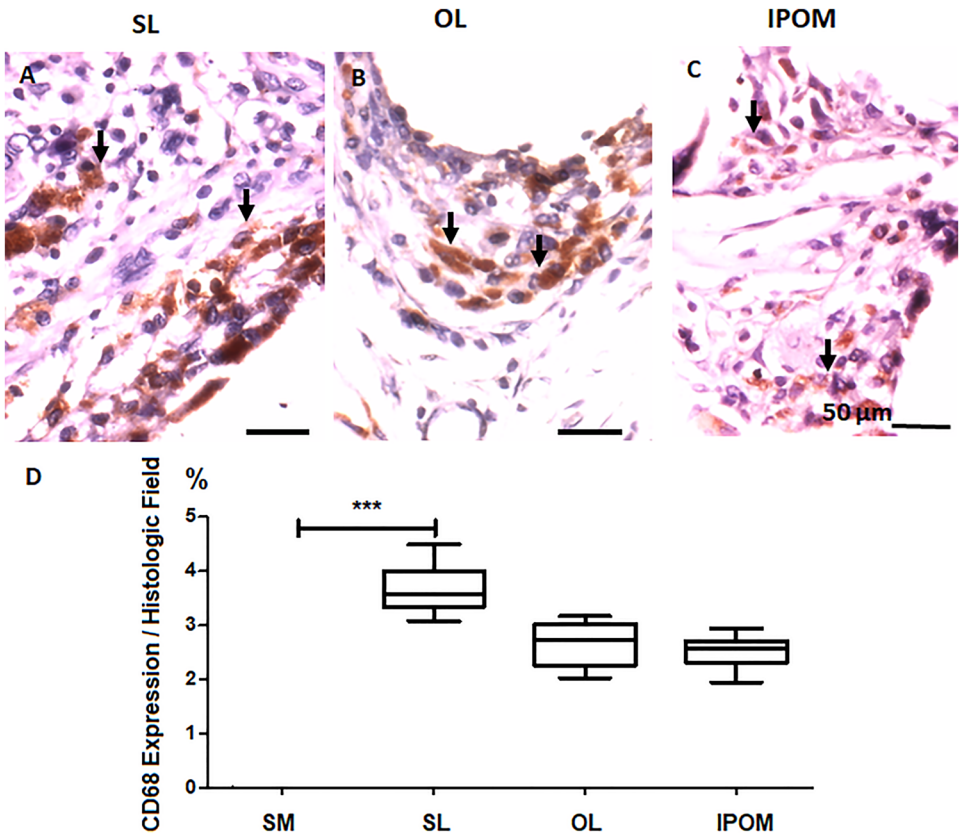

Fig. 8 CD 68 expression more abundant in sublay model. Sublay, Onlay, and IPOM models, (**A**), (**B**), and (**C**), respectively. 1:50 µm. **D** showing CD 68 expression between the groups

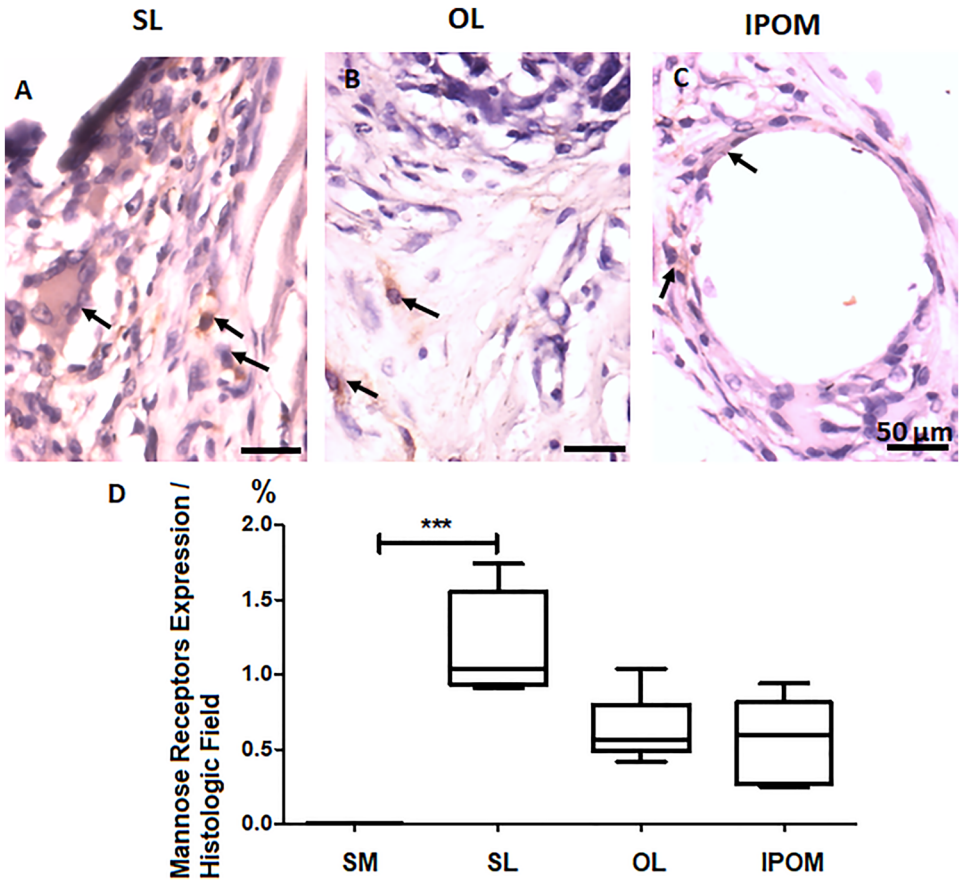

Fig. 9 Mannose receptors expression (arrows). Sublay, Onlay, and IPOM models, (**A**), (**B**), and (**C**), respectively. 1:50 µm. **D** showing mannose receptors expression throughout the groups

a SD of 0.26, in the SL group an average of 3.56%, with a SD of 0.47, in the OL group a mean of 2%, with a SD of 0.51, with a *p* value of 0.001 and in the SM group an average of 0.001%, with a SD of 0.4. When performing univariate multiple comparisons, we observed a global *p* of 0.0002 and a significant analysis only when comparing SM vs. SL group (Fig. 8).

Mannose receptors

Regarding the evaluation of the presence of mannose receptor markers, we visualized an average of 0.59% in the IPOM group, with a SD of 0.29; an average of 1.01%, with a SD of 0.8 in the SL group; an average of 0.56%, with a SD of 0.22 in the OL group; and an average of 0.0005% with a SD of also 0.0005 in the SM group. When performing univariate multiple comparisons on the values, we observed *p* values under 0.05 when only comparing SM vs. SL group, just like in the CD 68 evaluation and a global *p* of 0.005 regarding this analysis (Fig. 9).

iNOS

The analysis of iNOS receptors showed an average of 0.01% in the IPOM group, with a SD of 0.004; an average of 0.02%, with a SD of 0.004 in the SL group; an average of 0.004%, with a SD of 0.002 in the OL group; and an average of 0.0005% with a SD of also 0.0005 in the SM group. When performing univariate multiple comparisons on the values, we observed *p* values under 0.05 when comparing SM vs. SL, SM vs. OL, and SL vs. OL groups and a global *p* of 0.002 (Fig. 10).

Collagen density

The collagen density analysis demonstrated an average of 213.7% in the IPOM group, with a SD of 8.1, in the SL group an average of 223.9%, with a SD of 2.71 and in the OL group an average of 216%, with a SD of 1.59. The SM group did not show a significant value, therefore being excluded from this univariate comparison analysis. When performing univariate multiple comparisons on the values, we observed *p* values under 0.05 when comparing IPOM vs. SL and SL vs. OL groups and a global *p* of 0.0006 (Fig. 11).

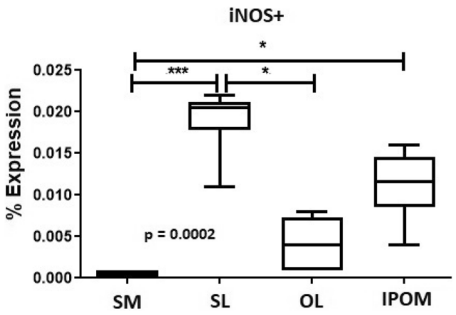

Fig. 10 Percentages of iNOS receptor expression

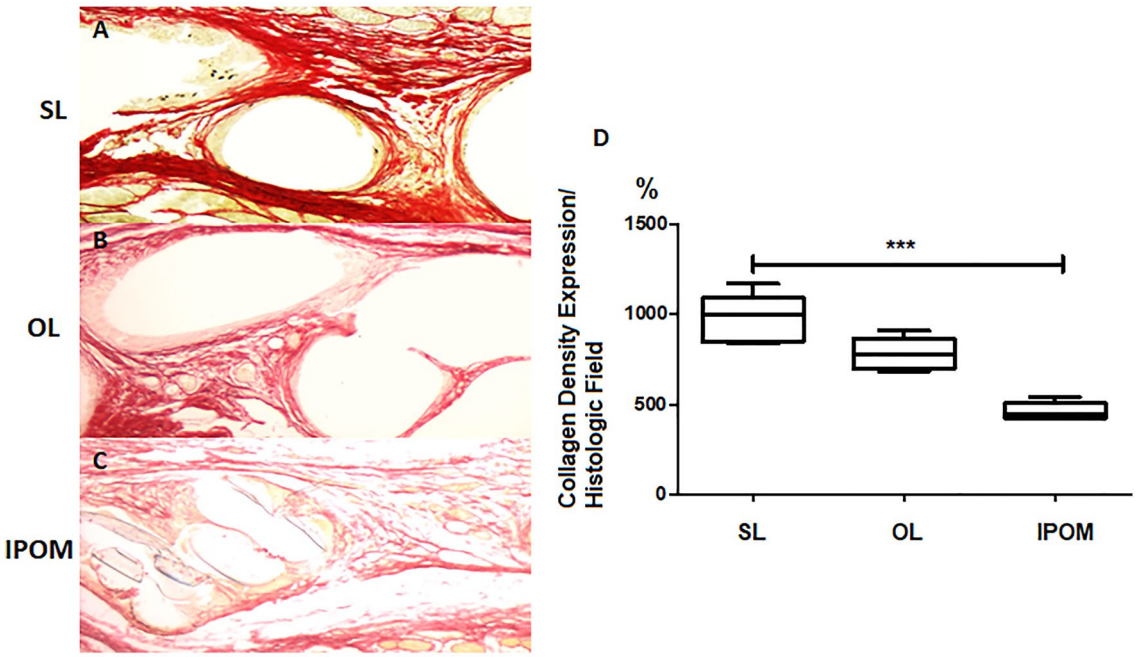

Fig. 11 Final aspect of collagen density deposition. Sublay, Onlay, and IPOM models, (**A**), (**B**), and (**C**), respectively. 1:200 µm. **D** represents the collagen density expression results

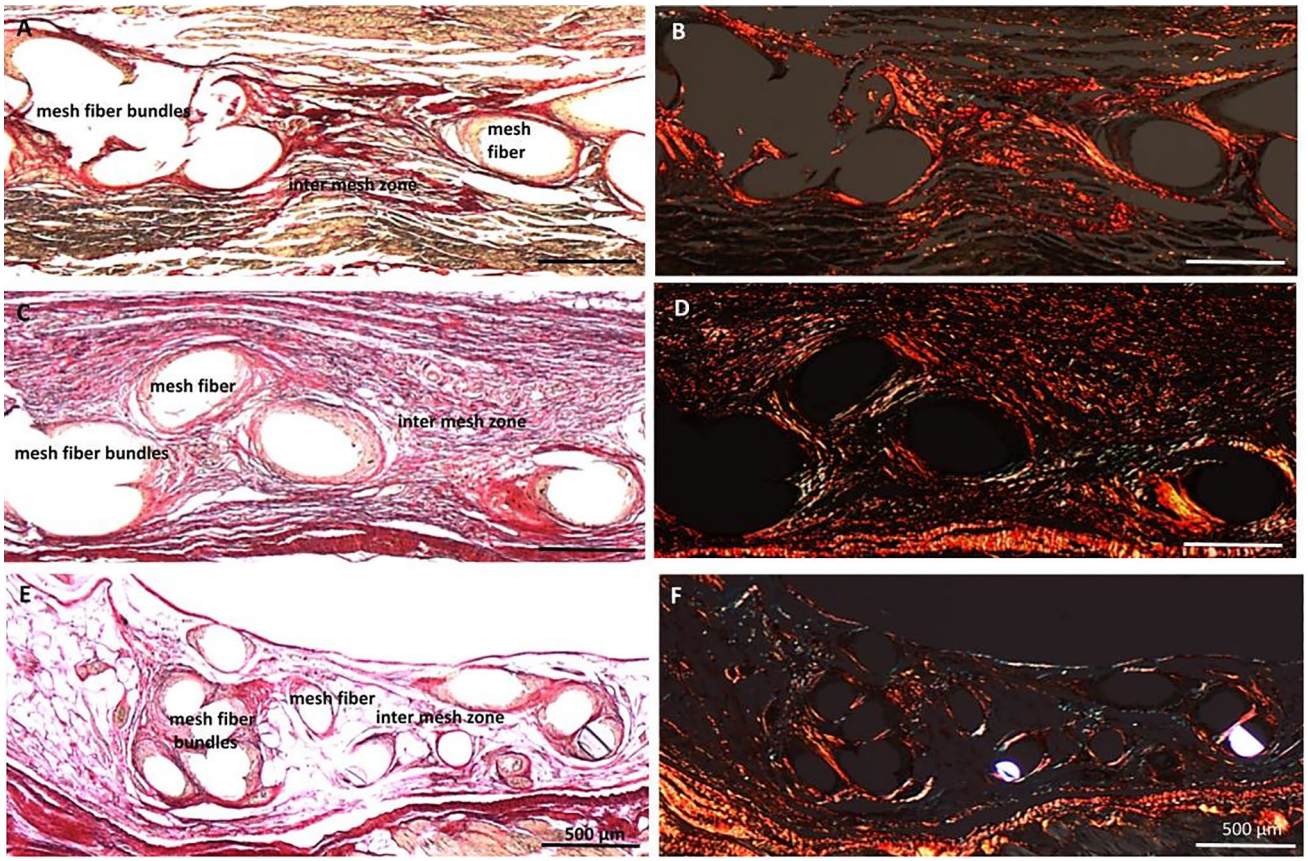

Fig. 12 Representative images from the abdominal wall containing the polypropylene meshes stained with *picrosirius* red visualized in light microscopy and polarized microscope (**A**, **C** and **E**: clear field and **B**, **D** and **F**: after polarization) at mesh implantation location. **A** and **B**: SL group, **C** and **D**: OL group; **E** and **F**: IPOM group). 1:100 µm

SL group showed in *picrosirius* sections a dense disposition of collagen fibers around mesh fibers or bundles as well as in the intermeshes spaces (Fig. 12A). Polarized images of *picrosirius*-stained sections revealed a predominance of red fibers (thick fibers), both around and in between mesh fibers (Fig. 12B). In contrast in OL groups, *picrosirius* stain demonstrated presence of thin collagen fibers disposed in intermeshes location as well as around mesh fibers (Fig. 12C). It was seen that polarization microscopy of *picrosirius* sections disclosed red fibers (thick fibers) disposed loosely around or inter meshes (Fig. 12D). In IPOM group, *picrosirius*-stained sections displayed a loose collagen network around mesh fibers or bundles (Fig. 12E) containing rare or sparsely disposed red fibers with almost absence of collagen deposed between mesh fibers or bundles (Fig. 12F).

Discussion

Surgical approaches for the treatment of incisional hernias are continuously advancing as innovative solutions arise and a more profound knowledge of the mechanisms behind repair is achieved. The use of meshes has been well established as advantageous in long-term outcomes, and now the debate has moved to other dilemmas such as what is the ideal method for approaching the defect, and in which abdominal wall layer should the mesh be placed. Several studies have shown that placement under the rectus abdominis muscle and over the posterior rectus sheath, i.e., the sublay or retrorectus technique, reduces rates of wound infection, recurrence, and early postoperative complications, without significantly increasing the risk of adhesion-related complications [9–11].

A clinical trial comparing primary suture, onlay and sublay techniques in primary prophylaxis of incisional hernias has also shown that the use of meshes is more efficient than primary suture; however, there was no statistically significant difference between onlay and sublay groups addressing development incisional hernias [18]. Nevertheless, given the short observation time and the fact that the study group was composed of subjects with no previous hernia, we believe the conclusions obtained from this study cannot be compared to the many clinical series confirming the superiority of sublay technique over onlay. Overall, it has

been demonstrated that sublay technique not only is equivalent to the classically used onlay technique in preventing the development of incisional hernias, but also superior to it in preventing hernia recurrence.

Even though these results by themselves have already caused an impact in the surgical community, with sublay repair being increasingly elected as the technique of choice in many specialized centers, and despite strong clinical evidence favoring sublay technique, the exact mechanism responsible for superiority is unknown. This fact encouraged our group to perform the experiments described above, since we believe they could be the first step toward characterization of the basic mechanism responsible for the superiority of one technique over another. The importance of this relies on prospects of continuous improvement in hernia treatment, since it lays a foundation for future endeavors in perfecting meshes and surgical techniques, based on the effect of the mesh on biological tissue and the influence of the surrounding microenvironment, as observed in our experiment. Aiming for this, our present study was designed to specifically evaluate the effect of mesh placement in different compartments of the abdominal wall, avoiding the interference of confounding factors, such as those related to the hernia itself. Hernias in humans are extremely complex and singular entities with a multitude of factors involved in their genesis, many of them related to the role of the abdominal wall in our bipedal stance, and this fact adds difficulty in obtaining an ideal animal hernia model. Moreover, the goal of this study was not to create true incisional hernias or to compare the efficacy of the techniques, since this has already been evaluated in clinical studies, but to characterize the effects of mesh placement on separate locations of the abdominal wall. Therefore, a model of laparotomy immediately followed by repair at the same surgical procedure was preferred over a true incisional hernia model.

The laparotomy model demonstrates the differences in fibrous tissue induced by mesh placement according to the different techniques studied, while also minimizing confounding factors that would be present if separate procedures were performed over time. The use of a true incisional hernia model, i.e., maintaining the defect after a laparotomy for weeks before correction, even though may mimic the pathophysiology of hernias, would interfere with the results of the study, as this model induces significant but variable formation of adhesions and other pathological features which would make the interpretation of the results much more difficult [16]. Considering the importance of translational results, we selected a high-weight polypropylene mesh, due to its widespread use for the treatment of hernias. Reasons for its vast use include low cost, easy access, effortless maneuverability, and the property of maintaining its tensile strength for an indeterminate period [19, 20]. This mesh induces a deep inflammatory reaction, resulting in appropriate incorporation into the tissues of the abdominal wall [21]. The fact that a mesh designed for humans has been used in 200–400 g rats may have implications on the degree of the inflammation and fibrogenesis observed. The weight, size of pores, and diameter of the polypropylene fibers are much larger for a rodent's size, which may lead to a more intense foreign body reaction. However, intergroup comparisons between the SL and OL groups have shown significant differences that should be attributed to the layer of the abdominal wall in which the mesh was placed, not to the type of mesh used, since it was the same for both groups. Besides, the choice of a mesh already used in current surgical practice makes these results more translatable to clinical medicine, unlike if a rat custom-made mesh had been used. This mesh can be used in different surgical techniques, improving outcomes without increasing the cost of the procedure.

Differential positioning of the mesh resulted in several measurable and statistically significant disparities detected after intergroup evaluations. One of the most prominent differences observed was concerning intra-abdominal adhesions. The IPOM group presented more adhesions, with all the animals had grade 3 or 4, whereas in SL 70% had grade 3 or 4 adhesions and the OL group had 60% grade 1 adhesions ($p < 0.0001$). Current literature supports our findings described in IPOM and OL group, as several studies have demonstrated that the positioning of a mesh in the cavity stimulates the adherence formation in any technique chosen and loose adhesions may arise after surgical corrections involving OL technique [15, 22, 23].

Nonetheless, this is the second descriptive study evaluating the presence of adhesions in an experimental model using SL technique [8]. Human studies, however, have not shown increased complications related to adhesions, such as intestinal obstruction, in patients submitted to SL technique. This apparent discrepancy may be due to the closer proximity of the mesh to the intraperitoneal space in rats, since their posterior rectus sheath is much thinner than that of a human. The greater inflammatory foreign body reaction caused by the heavier mesh, as discussed above, may also be a factor contributing to greater adhesion intensity in rats. Even though intense formation of adhesions may be a potential disadvantage of the SL model, there is no evidence indicating that this phenomenon also occurs in humans at levels high enough to be clinically significant and to cause adhesion-related complications. We ruled out the possibility that such adhesions were caused by preoperative or postoperative ruptures in the tissues separating the mesh from the peritoneal cavity by evaluating each adhesion individually and not finding any disruption of the posterior layer in our specimens.

Our hypothesis to explain the increased adhesion formation in SL group is based on mesh proximity to the

abdominal cavity, paracrine factors present in the compartment in which the mesh is inserted and more intense inflammatory reaction. Experimental studies with composite mesh used in intraperitoneal techniques have shown intense formation of adhesions [23], even though these meshes are specifically designed to be in direct contact with abdominal viscera, corroborating the assumption that the closer the inflammatory reaction is to the cavity, the greater the formation of adhesions. Besides, it is possible that polypropylene in contact with the aponeurotic and muscular fibers strongly induces collagen formation and recruitment of reparative elements to this compartment, leading to a greater induction of cell proliferation, and consequently more adhesions. Higher surgical trauma required to place the mesh in SL compartment may also contribute to greater extravasation of pro-inflammatory cytokines, leading to more intense inflammation and fibrogenesis.

Tension measurement is commonly used to estimate the progression of tissue healing. As days go by after the surgical repair, maximum tensile forces between tissues progressively decline until they reach a plateau. By the 30th day, tissues already have a uniformity of tension lines generated by aponeurosis healing, with or without mesh placement [24]. The presence of macroporous meshes results in greater tension between the structures in contact with the mesh. A study comparing distinct types of meshes and their tensiometric correlations in an experimental model concluded that macroporous meshes present higher levels of resistance in all phases [25], with increasing performance as the weeks passed.

Minimum tensile strength (MTS) required for mesh removal from its surrounding tissues in the abdominal wall is a good parameter to interpret the resistance of the repair, since recurrence is secondary to mesh displacement, and mesh resistance is by far greater than MTS. Additionally, MTS values varied uniformly between the groups. Two groups with mesh placement (SL and OL) displayed greater MTS than SM group, which indicates that following mesh repair, aponeurotic-induced fibrogenesis itself is not the only mechanism responsible for healing and strengthening of the abdominal wall. However, the IPOM displayed a poor result of MTS, demonstrating that there was no resistance whatsoever between the abdominal wall ($p < 0.0001$).

Neovascularization induced by the presence of mesh and by surgical trauma itself also has a significant role in determining final tensile strength, because the greater the suture tension for tissue synthesis, the greater the chance of local ischemia, leading to alterations in collagen and fibroblast proliferation [26]. The amount and quality of collagen formed is particularly important as well, since the formation of denser, more cohesive bands of collagen results in a greater force required to rupture the tissue.

Among groups in which the mesh was employed, SL specimens required a much greater MTS in comparison to all the groups, indicating a higher tensile strength in the former group. In fact, after statistical analysis, OL group showed no significant difference in tensile strength compared to SM. Higher MTS observed after SL repair is likely due to the formation of a better-quality fibrous tissue, as fibrogenesis in this group appears to be more cohesive and mature, resulting in a more consistent fixation of the mesh. Those findings are compatible with the conclusion of several clinical studies reporting lower recurrence rates using SL technique [9–11]. In this line of thought, one could argue that such difference in fibrogenesis among the three techniques could be related to the different cellular composition of each of the abdominal wall compartments. Adipose tissues have the capacity of modulating inflammation and, therefore, could be involved in reducing fibrogenesis following OL repair [27]. At the same time, the posterior rectus abdominis sheath appears to be a more favorable environment for the development of an optimized fibrous tissue.

Histological and immunohistochemical analysis of all groups revealed involvement of the same type of tissue repair, characterized by the predominant presence of a chronic granulomatous inflammatory process induced by polypropylene, with Langhans giant cell and foreign body giant cell formation, associated with variable sparse or aggregated histiocyte proliferation.

In the three main models (IPOM, SL, and OL), the substrate profile is compatible with the intermediate proliferative phase of inflammation, although a great heterogeneity in such staging was observed, even within a single area. Considering this, we assume collagen deposition and maturation are variable, gradual, and heterogeneous processes evaluated across specimens. We believe those results from the fact that collagen biosynthesis depends on the type and location of the abdominal wall injury.

Concentrations of repair elements throughout the wounds of rats from OL group were more homogeneously distributed, probably due to the uniformity of mesh placement on the abdominal wall, causing less trauma to tissue structure and, therefore, less inflammatory and reparative responses. In this model, the distribution of the constitutive elements of repair was less variable, and resulted in bimodal curves of collagen deposition, and no major variation of the other components. This group also presented comparatively high concentrations of fibroblasts and neovascularization. This may translate into a more advanced maturation phase of the repair process in these cases, favoring deposition of neocollagen over inflammatory or proliferative elements, resulting in a more uniformly organized fibrous tissue.

The histological analysis of SL group demonstrated with higher densities of inflammatory elements, such as polynucleated cells and myeloid progenitors. Indeed, previously it

was characterized that the myeloid cells cause a persistent inflammation after implantation of polypropylene meshes. CD68 is routinely used as a histochemical marker of cells of the macrophage lineage such as monocyte/macrophages [28], multinucleated giant cells, and other tissue resident macrophages [29, 30], but not in dendritic cells [31]. CD68 can be significantly upregulated in macrophages responding to inflammatory stimuli [32, 33], and therefore is considered as a marker of activated macrophage [34]. Previous studies have demonstrated that the macrophages participating in implanted polypropylene meshes are $CD68^{+}$ macrophages [34–36].

Macrophages are a heterogeneous population of cells that are activated/polarized by microenvironmental cues toward distinct functional phenotypes: the pro-inflammatory M1 phenotype or an anti-inflammatory M2 phenotype. The M1 phenotype is classically associated with pro-inflammatory host defense functions such as antimicrobial activity and phagocytosis, serving as immune effectors whereas the alternatively activated M2 phenotype is involved with various tissue remodeling responses including resolution of inflammation and wound healing [37]. In the normal wound-healing process, M1 macrophages appear first to clean the injured site, followed by M2 macrophages to complete the wound-healing process; furthermore, in general, immune responses exhibit a mixed population of the two phenotypes with a preferred ratio. That is, a high M1/M2 ratio develops first, and a low M1/M2 ratio develops later to regenerate the tissues.

Implantation of surgical meshes in experimental studies in animals have demonstrated that at least within 12 weeks after implantation, mainly M1 macrophages surrounded the mesh fibers and formed the foreign body granuloma [38, 39]. Similarly, but in humans, the implantation of a lightweight, wide-pore polypropylene mesh used for repair of pelvic organ prolapse and stress urinary incontinence also showed the predominance of the M1 subtype, with significant increase of M1 and M2 cytokines/chemokines, MMP-9 (pro- and active), and MMP-2 (active) in explanted meshes [40].

In humans, the interface of the polypropylene surgical meshes in the abdomen about 60% of macrophages had an M2 phenotype whereas only 6% had an M1 phenotype [41]. Besides that, these authors observed that the M2 response was accompanied by abundant collagen deposition, and fibrosis. Collagen type I was deposed directly at the interface to the meshes where percentage of M2 was highest while collagen III was in zones distant from the mesh at places poor in M2 macrophage [41]. The co-localization of macrophages with type I collagen especially at the mesh–tissue interface (> 50%) could indicate that M2 macrophages are responsible for collagen I degradation via a mannose receptor mediated (CD206) pathway after MMP cleavage[37]. Additionally, macrophages may be involved in the synthesis of collagen I, since the synthesis of other collagen types has been demonstrated in animals and humans [42, 43].

Implantation of biomaterials in the body is accompanied by immune responses formed against biomaterials themselves, and against tissue injuries that occur during implantation, and include acute and chronic inflammation, and foreign body reactions. Multinucleated giant cells (MNGCs) appear when macrophages are unable to phagocytose biomaterials because of their size. Therefore, they fuse together to form MNGCs, and they release cytokines that are different from the cytokine-release profiles of the M1 and M2 macrophages and produce reactive oxygen species, which can damage implanted biomaterials. Furthermore, it was previously shown that MNGCs express M1 (TNF-α, iNOS, and IL-1β) and M2 (IL-10 and Arg1) markers [44]. Indeed, this study showed that IPOM group induced the highest level of MNGCs, and presence of plasma cells. It could be hypothesized that the ongoing activity of these cells in degrading the membranes could elicit the formation of plasma cells.

Therefore, we conclude that in rats, mesh positioning in sublay compartment is associated with the development of more pronounce minimum tensile force required for detaching the surrounding abdominal wall tissues it was incorporated. The intensity of these findings correlates to the different histological and immunohistochemical profiles observed following each repair, since SL group was characterized by a higher proportion of collagen, inflammatory and reparative elements. These findings are related to a different profile of cellular and molecular elements, associated to optimized cicatrization process. Characterizing these pro-healing elements and its counterparts will allow the development of new therapeutic tools which could be added to the still far-from-ideal current therapeutic options for IH treatment. Further studies are necessary to improve our knowledge about this subject, especially regarding the cellular mechanisms involved in fibrogenesis induced by mesh positioning in various parts of the abdominal wall.

Declarations

Conflict of interest Fernando Ponce Leon, Christina Takyia, Juliana da Costa and José Eduardo Manso declare that they have no conflict of interest.

Ethical approval Animal studies experimental protocol was submitted to the Ethics Committee for the Use of Animals in Scientific Experimentation of the Health Sciences Center of the Universidade Federal do Rio de Janeiro (CEUA-CCS), registered in the National Council for the Control of Animal Experimentation (CONCEA) under process number 01200.001568/2013-87, and received approval for execution. The guidelines for the use and care of laboratory animals were done and followed by the authors, respecting animal rights.

Informed consent For this type of study informed consent is not required.

References

1. Millikan KW (2003) Incisional hernia repair. Surg Clin N Am 83:1223–1234
2. den Hartog D, Dur AH, Tuinebreijer WE, Kreis RW (2008) Open surgical procedures for incisional hernias. Cochrane Database Syst Rev 3:CD006438
3. Luijendijk RW, Hop WCJ, van den Tol P, de Lange DCD, Braaksma MMJ, Ijzermans JNM, Boelhouwer RU, de Vries BC, Salu MKM, Wereldsma JCJ, Bruijninckx CMA, Jeekel J (2010) A comparison of suture repair with mesh repair for incisional hernia. N Engl J Med 343(6):392–398
4. Burger JW, Luijendijk RW, Hop WC, Halm J, Verdaasdonk EG, Jeekel J (2004) Long-term follow-up of a randomized controlled trial of suture versus mesh repair of incisional hernia. Ann Surg 240(4):578–583
5. Biondo-Simões MLP, Morais CF, Tocchio AFZ, Miranda RA, Moura PAP, Colla K, Robes RR, Ioshii SO, Tomasich FDS (2016) Characteristics of the fibroplasia and collagen expression in the abdominal wall after implant of the polypropylene mesh and polypropylene/polyglecaprone mesh in rats. Acta Cir Bras 31:294–299
6. Nursal TZ, Hamalogku E (1999) Insizyonel herniler. T Klin Cerrahi 4:182–187
7. Batkir A, Dogru O, Girgin M, Aygen E, Kanat BH, Dabak DO, Kuloglu T (2013) The effects of different prosthetic materials on the formation of collagen types in incisional hernia. Hernia 17:249–253
8. Ponce Leon F, Manso JEF, Abud VL, Nogueira W, Silva PC, Martinez R (2018) Sublay repair results in superior mesh incorporation and histological fibrogenesis in comparison to onlay and primary suture in an experimental rat model. Hernia 22(6):1089–1100. https://doi.org/10.1007/s10029-018-1808-y. (**Epub 2018 Aug 27 PMID: 30168008**)
9. Albino F, Patel K, Nahabedian M, Sosin M, Attinger C, Bhanot P (2013) Does mesh location matter in abdominal wall reconstruction. A systematic review of the literature and a summary of recommendations. Plast Reconstr Surg 132(5):1295–1304
10. Hawn M, Snyder C, Graham L, Gray S, Finan K, Vick C (2010) Long-term follow up of technical outcomes for incisional hernia repair. J Am Coll Surg 210(5):648–655
11. Holihan JL, Nguyen DH, Nguyen MT, Mo J, Kao LS, Liang MK (2016) Mesh location in open ventral hernia repair: a systematic review and network meta-analysis. World J Surg 40:89
12. Chevrel JP (1979) The treatment of large midline incisional hernias by "overcoat" platy and prothesis (author's transl). Nouv Presse Med 8(9):695–696
13. Rivers J, Lardennois B, Pire JC, Hibon J (1973) Large incisional hernias. The importance of flail abdomen and of subsequent respiratory disorders. Chirurgie 99(8):547–563
14. Neligan P, Peter C (2015) Plastic surgery: principles, 3rd edn. Elsevier, Rio de Janeiro, pp 240–252
15. Ricciardi BF, Chequim LH, Gama RR, Hassegawa L (2012) Correction of abdominal hernia with mesh tissue—study in Wistar rats. Rev Col Bras Cir 39(3):195–200
16. Dolber PC, Spach MS (1993) Conventional and confocal fluorescence microscopy of collagen fibers in the heart. J Histochem Cytochem 41:461–469
17. Chia CY, Medeiros AD, Corraes AMS, Manso JEF, Silva CSCD, Takiya CM, Vanz RL (2018) Healing effect of andiroba-based emulsion in cutaneous wound healing via modulation of inflammation and transforming growth factor beta 31. Acta Cir Bras 33(11):1000–1015
18. Jairam AP, Timmermans L, Eker HH, Pierik R, van Klaveren D, Steyerberg EW et al (2017) Prevention of incisional hernia with prophylactic onlay and sublay mesh reinforcement versus primary suture only in midline laparotomies (PRIMA): 2-year follow-up of a multicentre, double-blind, randomized controlled trial. Lancet 390(10094):567–576
19. Klosterhafen B, Junge K, Hermanns B, Klinge U (2002) Influence of implantation interval on the long-term biocompatibility of surgical mesh. Br J Surg 89:1043–104818
20. Morris-stiff GJ, Hughes LE (1998) The outcomes of nonabsorbable mesh placed within the abdominal cavity: literature review and clinical experience. J Am Coll Surg 186:352–367
21. van't Riet M, Burger JW, Bonthuis F, Jeekel J, Bonjer JH (2004) Prevention of adhesion formation to polypropylene mesh by collagen coating. A randomized controlled study in a rat model of ventral hernia repair. Surg Endosc 18:681–685
22. Sergent F, Desilles N, Lacoume Y, Tuech J, Marie J, Bunel C (2010) Biomechanical analysis of polypropylene prosthetic implants for hernia repair: an experimental study. Am J Surg 200:406–41221
23. Voskerician G, Jin J, Hunter S, Williams C, White M, Rosen M (2009) Human peritoneal membrane reduces the formation of Hernia 1 3 intra-abdominal adhesions in ventral hernia repair: experimental study in a chronic hernia rat model. J Surg Res 157:108–114
24. Akinci M, Ergul Z, Kantarcioglu M, Tapan S, Ozier M, Gunal A, Kulacoglu H, Ide T, Sayal A, Eryilmaz M, Kozak O (2014) The effect of relaparotomy timing on wound healing in an animal model. Int J Surg 12:1434–1438
25. Utrabo C, Czeczko N, Busato C, Montemór-Netto M, Lipinski L, Malafaia, (2017) Tensiometric analysis of meshes used in abdominal ventral wall defects in rats. Arq Bras Cir Dig 30(3):165–168
26. Schachtrupp A, Wetter O, Höer J (2016) An implantable sensor device measuring suture tension dynamics: results of developmental and experimental work. Hernia 20:601–606
27. Itman A, Khalek F, Alt E, Butler C (2010) Adipose tissue derived stem cells enhance bioprosthetic mesh repair in ventral hernias. Plast Reconstr Surg 126(3):845–854
28. Ferenbach D, Hughes J (2008) Macrophages and dendritic cells: what is the difference? Kidney Int 74:5–7
29. Brooks E, Simmons-Arnold L, Naud S et al (2009) Multinucleated giant cells' incidence, immune markers, and significance: a study of 172 cases of papillary thyroid carcinoma. Head Neck Pathol 3:95–99
30. Bobryshev YV (2006) Monocyte recruitment and foam cell formation in atherosclerosis. Micron 37:208–222
31. Betjes MG, Haks MC, Tuk CW et al (1991) Monoclonal antibody EBM11 (anti-CD68) discriminates between dendritic cells and macrophages after short-term culture. Immunobiology 183:79–87
32. O'Reilly D, Quinn CM, El-Shanawany T et al (2003) Multiple Ets factors and interferon regulatory factor-4 modulate CD68 expression in a cell type-specific manner. J Biol Chem 278:21909–21919
33. Rabinowitz SS, Gordon S (1991) Macrosialin, a macrophage-restricted membrane sialoprotein differentially glycosylated in response to inflammatory stimuli. J Exp Med 174:827–836
34. Bryan N, Ashwin H, Chen R, Smart NJ, Bayon Y, Wohler S, Hunt JA (2016) Evaluation of six synthetic surgical meshes implanted subcutaneously in a rat model. J Tissue Eng Regen Med 10(10):E305–E315
35. Wolf MT, Dearth CL, Ranallo CA, LoPresti S, Carey LE, Daly KA, Brown BN, Badylak SF (2014) Macrophage polarization in response to ECM coated polypropylene mesh. Biomaterials 35(25):6838–6849
36. Heymann F, von Trotha K-T, Preisinger C, Lynen-Jansen P, Roeth AA, Geiger M, Geisler LJ, Frank AK, Conze J, Luedde T, Trautwein C, Binnebösel M, Neumann UP, Tacke F (2019) Polypropylene mesh implantation for hernia repair causes myeloid

cell–driven persistent inflammation. JCI Insight 4(2):e123862. https://doi.org/10.1172/jci.insight.123862
37. Madsen DH, Leonard D, Masedunskas A et al (2013) M2-like macrophages are responsible for collagen degradation through a mannose receptor–mediated pathway. J Cell Biol 202:951–966. https://doi.org/10.1083/jcb.201301081
38. Brown BN, Mani D, Nolfi AL et al (2015) Characterization of the host inflammatory response following implantation of prolapse mesh in rhesus macaque. Am J Obstet Gynecol 213:668.e1-668.e10. https://doi.org/10.1016/j.ajog.2015.08.002
39. Wolf MT, Dearth CL, Ranallo CA et al (2014) Macrophage polarization in response to ECM coated polypropylene mesh. Biomaterials 35:6838–6849. https://doi.org/10.1016/j.biomaterials.2014.04.115
40. Nolfi AL, Brown BN, Liang R et al (2016) Host response to synthetic mesh in women with mesh complications. Am J Obstet Gynecol 215:206.e1-206.e8. https://doi.org/10.1016/j.ajog.2016.04.008
41. Dievernich A, Achenbach P, Davies L, Klinge U (2020) Tissue remodeling macrophages morphologically dominate at the interface of polypropylene surgical meshes in the human abdomen. Hernia 24:1175–1189
42. Simões FC, Cahill TJ, Kenyon A et al (2020) Macrophages directly contribute collagen to scar formation during zebrafish heart regeneration and mouse heart repair. Nat Commun 11:600. https://doi.org/10.1038/s41467-019-14263-2
43. Schnoor M, Cullen P, Lorkowski J et al (2008) Production of type VI collagen by human macrophages: a new dimension in macrophage functional heterogeneity. J Immunol 180:5707–5719
44. Moore LB, Sawyer AJ, Charokopos A, Skokos EA, Kyriakides TR (2015) Loss of monocyte chemoattractant protein-1 alters macrophage polarization and reduces nfkappab activation in the foreign body response. Acta Biomater 11:37–47